ISSN 0022-4766, Journal of Structural Chemistry, 2023, Vol. 64, No. 4, pp. 584-594. © Pleiades Publishing, Ltd., 2023.
Russian Text © The Author(s), 2023, published in Zhurnal Strukturnoi Khimii, 2023, Vol. 64, No. 4, 108770.

STRUCTURAL STABILIZATION OF D- AND T-CAGES OF THE sI HYDRATE BY GAS MOLECULES

M. B. Yunusov[1]* and R. M. Khusnutdinov[1,2]

Mechanisms of structural stabilization of sI hydrates by CH_4, H_2S, H_2, N_2, Ar, Kr, Xe, CO_2, C_2H_6, C_3H_6 gas molecules are studied by the density functional method. It is shown that the hydrate D- and T-cages are deformed and their radii are changed (up to –0.23%) upon the introduction of guest gas molecules. Binding energies of the gases in the D- and T-cages are calculated. It is established that molecules with diameters $d < 5$ Å and $d > 5$ Å stabilize better D- and T-cages, respectively. Two groups of gases can be distinguished, depending on the binding energy dependence on the molecule's mass: molecular gases ($dE_b/dM \in$ (–0.008; –0.006) eV·mol/g) and atomic gases ($dE_b/dM \in$ (–0.002; –0.0015) eV·mol/g). It is shown that the orientation of extended CO_2, C_2H_6, and C_3H_6 molecules along the long axis of the T-cage is most energetically favorable. Densities of electronic states $N(E)$ are calculated for the unfilled sI hydrate and for sI hydrates containing CH_4 and CO_2. It is shown that the presence of a guest molecule decreases the energy of the electronic subsystem and increases the hydrate's stability.

DOI: 10.1134/S0022476623040066

Keywords: gas hydrates, ab initio, binding energy, density of electronic states.

INTRODUCTION

Highly interesting compounds, gas hydrates, are formed on Earth in permafrost zones, on ocean shelves, under conditions of low temperatures, high pressures, presence of water, and sufficient concentration of low molecular gases [1]. The hydrates are a crystal lattice of water molecules with cages of various shapes. Upon the nucleation of hydrates, gases molecules with a diameter of 4-7 Å can be incorporated into the water clusters. Hydrates containing natural gases (CH_4, C_2H_6, C_3H_8) are of particular interest as potential new sources of hydrocarbon energy [2]. Most hydrates existing in nature have the sI crystal structure containing two types of cages, D and T (Fig. 1). According to various estimates, the Earth's interior contains at least 10^{16} m^3 of natural gas in the form of hydrates. These huge reserves are not only an economically useful resource, but also a cause for concern, because some part of gas from hydrates can be released into the atmosphere as a result of natural disasters such as earthquakes or volcanic eruptions and lead to irreversible climatic changes. Besides, the gas industry is concerned about the problem of hydrate formation in gas pipelines and wells [1, 3]. The hydrates are accumulated on pipe walls, plug them up and reduce the efficiency of production. One factor increasing the interest in

[1]Kazan (Volga region) Federal University, Kazan, Russia; *mukhammadbek@mail.ru. [2]Udmurt Federal Research Center, Ural Branch, Russian Academy of Sciences, Izhevsk, Russia. Original article submitted February 4, 2023; revised February 28, 2023; accepted March 1, 2023.

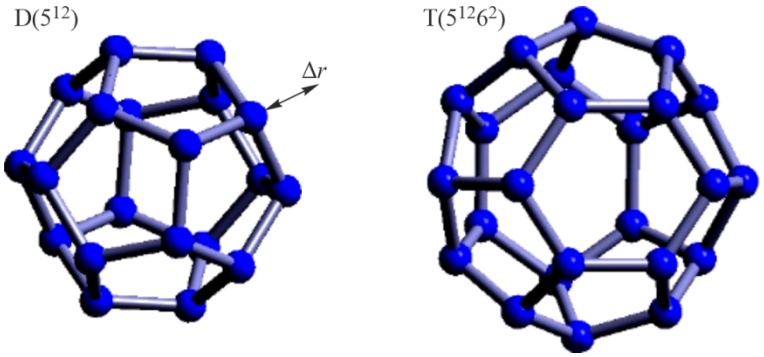

Fig. 1. D- and T-cages of hydrates. The nodes are oxygen atoms, the edges are formed by hydrogen bonds (m^n - n faces with m edges).

clathrate systems is their ability to contain large gas volumes. For example, 1 m^3 of hydrate can contain up to 160 m^3 of methane [4]; therefore, these substances can be used for the storage and transportation of gases such as hydrogen [5].

Thermodynamic properties, phase diagrams, equations of state, structural and mechanical properties of hydrates have been quite well studied experimentally and theoretically; the key studies in this field were reported in [6-14]. The authors of [15] proposed an original thermodynamic model of clathrate compounds to study stability regions of crystalline phases in water–hydrogen system, including hydrates. Numerous works have been devoted to the study of hydrate nucleation processes. [16-20]. It was shown that a system consisting of water and gas in sufficient concentration passed through a series of amorphous states resulting in small water clusters in the form of rings and cups, which combine into molecular cages capturing gas molecules. The authors of [21] studied the rearrangement of a hydrogen bond network of liquid water into the crystal lattice of methane hydrate and showed that hydrate nucleation can proceed simultaneously in the entire solution volume.

The lack of accurate first-principle studies of electronic and energy features of hydrates becomes obvious against the background of the study of structural, thermophysical, and kinetic properties of clathrate systems. In particular, there is lack of studies of the mechanisms of stabilization of hydrates by guest molecules and the effect of gas molecules on the surrounding water framework in terms of electronic states. To date, few first-principle studies of hydrate systems taking into account electronic degrees of freedom have been reported. Thus, the authors of [22] calculated binding energies for H_2, CH_4, CO, CO_2 gases as part of the sI hydrate and obtained densities of electronic states $N(E)$ for molecules forming the D-cage in the presence and in the absence of guest gas molecules. The authors of [23] obtained and analyzed components of the density of electronic states $N(E)$ and dielectric functions of the sI methane hydrate for three cases: both cages filled; no methane in the D-cage; no methane in the T-cage. It was shown that the absence of methane in the small D-cage has little effect on the crystal structure, while its in the large T-cage causes significant deformation of the crystal lattice and decreases the stability of the hydrate. In [24], the density functional theory was applied to study the stability of T- and H-type water cages containing 18 alkane compounds, including methane, ethane, and cyclopropane. In [25], various DFT functionals were used to calculate binding energies and the energies of deformation of D-, T-, and H-cages with incorporated sulfur-containing (H_2S, CS_2) and nitrogen-containing (N_2, NO, NH_3) molecules. The authors of [26, 27] reported a DFT simulation of the sI hydrate lattice and obtained the density of electronic states $N(E)$ and the band structure $E(\mathbf{k})$ for this type of hydrate.

The purpose of this work is to study the influence of incorporated gases H_2, N_2, Ar, Kr, Xe, CO_2, H_2S, CH_4, C_2H_6, C_3H_6 on molecular cages of clathrate hydrates and to reveal the mechanisms of stabilization of clathrate systems by guest molecules. To this aim, we conducted a DFT simulation of clathrate sI systems containing these gases, calculated binding energies of gas molecules in D- and T-type cages, estimated the deformation of the cages in the presence of various guest molecules, calculated and analyzed the densities of electronic states $N(E)$ of the water lattice in the presence and in the absence of gas molecules.

STRUCTURE OF sI HYDRATES

Clathrate hydrates contain several standard types of water cages whose combinations provide the structural diversity of these crystalline nonstoichiometric compounds [28-32]. The type of resulting hydrate is affected by external thermobaric conditions and characteristics of the hydrate-forming molecule. The cubic sI structure (Fig. 2) is most interesting, since it is most common met in nature, and hydrates of methane and ethane (potential sources of fuel) have the sI structure. The sI unit cell is a framework of 46 water molecules and consists of two D-cages ($r \approx 3.9$ Å) and six T-cages ($r \approx 4.4$ Å) (Fig. 1).

Cages in clathrate hydrates are polyhedrons with oxygen atoms at the vertices "bonded" to each other due to the ability of water molecules to form hydrogen bonding, a particularly strong type of intermolecular bonding [33-35]. It was determined that the lattice parameter for the sI structure is equal to 12.03 Å [36]. The authors of the study calculated lattice parameters of sI, sII, and sH hydrates by the Monte Carlo method using the Bernal–Fowler rules [37]. The composition of hydrates is variable and depends on the cage occupancies. In the general case, it is described by the formula $M{\cdot}n{\cdot}H_2O$, where M is a gas molecule; n is the average number of water molecules per gas molecule (hydrate number). Small gas molecules (less than 5 Å in diameter) in the composition of the sI hydrate, are characterized by the hydration number $n \approx 6$, meaning that almost all cages are filled. For gases with large molecules (more that 5 Å in diameter), the hydrate number is $n \approx 7.7$, meaning that only large T-cages are filled. Gases CH_4, H_2S, CO_2, C_2H_6, C_3H_6 form the sI structure, while gases H_2, N_2, Ar, Kr usually form the sII structure; and D-cages are filled in both cases. Under high pressures, sII hydrates can transform into the sI phase [6]. Taking into account the data on the occupancy of hydrates presented in [6-14], we conducted DFT calculations of unit cells of the sI hydrate containing CH_4, H_2S, H_2, N_2, Ar, Kr, Xe gas in D- and T-cages and CO_2, C_2H_6, C_3H_6 gases in T-cages.

COMPUTATIONAL DETAILS

The ab initio calculations were conducted using the specialized VASP package within the density functional (DFT) method [38-41]. In this method, transition is made from the wave functions to the electron density (1), and then a system of Kohn–Sham equations (2) is solved while taking into account the effective one-electron self-consistent potential (3):

$$n(r) = \sum_{i\sigma} |\psi_{i\sigma}(r)|^2, \quad (1)$$

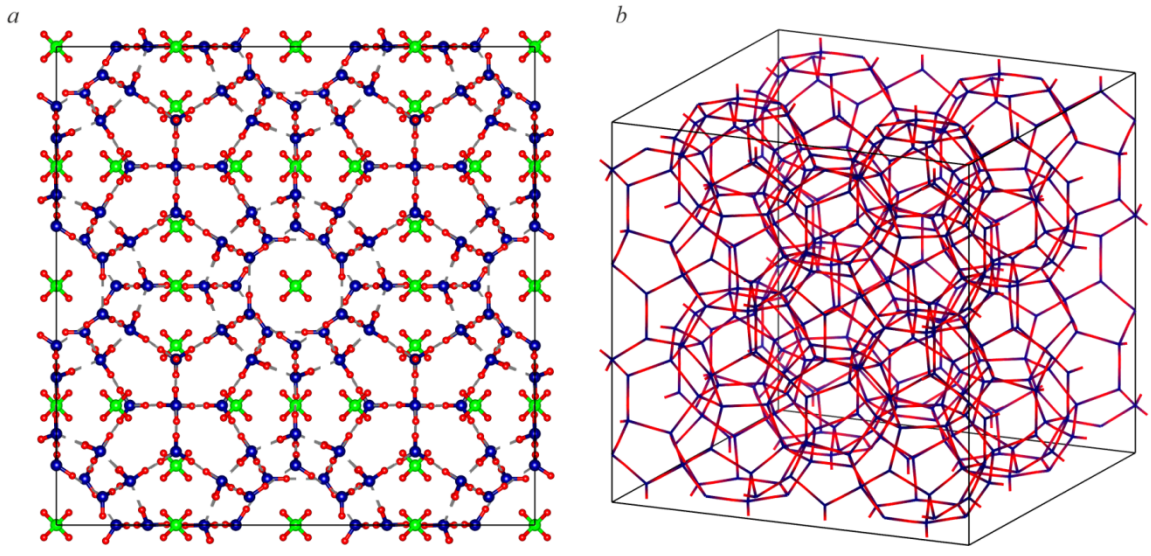

Fig. 2. Crystal lattice of the sI methane hydrate: oxygen (blue balls), carbon (green balls), hydrogen (red balls) (see the electronic version).

$$\left(-\frac{1}{2}\nabla^2 + V_{eff}(r)\right)\psi_{i\sigma}(r) = \varepsilon_{i\sigma}\psi_{i\sigma}(r), \tag{2}$$

$$V_{eff}(r) = V_{ext}(r) + V_H(r) + V_{XC}(r) = V_{ext}(r) + \int \frac{n(r')}{|r - r'|}dr' + \frac{\delta E_{XC}[n(r)]}{\delta n(r)}. \tag{3}$$

In the present study, we used the PBE exchange-correlation functional in the generalized gradient approximation (GGA) [42]; this functional takes into account the inhomogeneity of electron density distribution and is more accurate than the standard local density approximation (LDA) [39]. As a non-local correlation effect, the van der Waals interaction (that should occur between the clathrate water lattice and the guest molecule) is indirectly taken into account in GGA-based potentials in the exchange-correlation energy $E_{xc}[n(r)]$ [43]. Note that powerful functionals such as VdW-DF directly taking into account the Van der Waals interaction have already been developed [44]. The ion-electron interaction was calculated with the PAW potential [45]. The basis set consisted of plane waves with energies less than 345 eV. The simulation was conducted for the system's ground state using periodic boundary conditions. After placing gas molecules in water cages, an optimization procedure was performed using the RMM-DIIS algorithm [46] to achieve an energy convergence of 10^{-4} eV. The following hydrate systems were simulated: sI cell with empty molecular cages, sI cell with gas in the D-cage, sI cell with gas in the T-cage. The guest molecules were the following compounds that are most often met in gas hydrates: CH_4, H_2S, H_2, N_2, Ar, Kr, Xe, CO_2, C_2H_6, C_3H_6.

EFFECT OF GUEST MOLECULES ON THE CAGE GEOMETRY

Analysis of the geometry of unfilled sI lattices and sI lattices with guest gases showed that gases in the hydrate crystal lattice cause deformation of D- and T-cages (Fig. 1). We calculated the changes that distances from the center of a cage to its vertices undergo upon the introduction of various gas molecules. Fig. 3 shows relative changes of Δr radii for each node of D- and T-cages filled with different gases. Table 1 lists average changes of Δr radii of D- and T-cages.

According to the data presented in Fig. 3 and Table 1, the presence of gas in the clathrate lattice most often decreases the volume of cages due to the interaction between the atoms of the surrounding cage and the central gas molecule. The intermolecular interaction between gas and water molecules of the surrounding cage increases the stability and the thermodynamic stability of the hydrate, while the unfilled clathrate lattice is metastable. In the case of a hydrogen molecule in a D-cage, the cage radius increases slightly by +0.06%. This may indicate that one hydrogen molecule cannot completely stabilize the D-cage. According to the results of [47], clusters of 2-4 hydrogen molecules can be introduced into the cages to stabilize natural gas hydrates. Large CH_4, H_2S, and Kr molecules most strongly affect D-cages, while the influence of H_2, N_2,

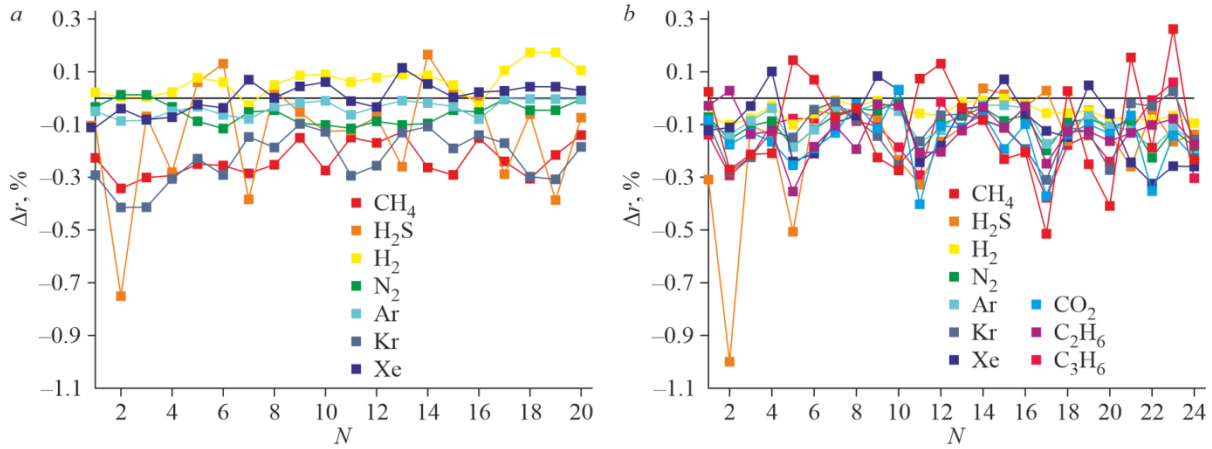

Fig. 3. Relative changes in distance Δr from the center to the nodes of cages D (*a*) and T (*b*) upon the introduction of different gases.

TABLE 1. Average Changes of Cages Radii (Δr, %) of the sI Hydrate in the Presence of Various Guest Molecules

Gas	Cage	
	D	T
CH_4	–0.23	–0.14
H_2S	–0.13	–0.17
H_2	+0.06	–0.05
N_2	–0.06	–0.11
Ar	–0.04	–0.10
Kr	–0.23	–0.13
Xe	+0.00	–0.10
CO_2	–	–0.16
C_2H_6	–	–0.13
C_3H_6	–	–0.11

Ar, and Xe molecules on the D-cage radius does not exceed –0.06%. All the considered gases reduce the T-cage radius by –0.10…–0.17%, only the influence of hydrogen does not exceed –0.05%. In [25], relative changes of D- and T-cages radii upon the introduction of N_2 molecules were –0.12% and –0.57%. The values obtained in the present work are –0.06% and –0.11%. Changes in the radii of D- and T-cages upon the introduction of H_2S were found equal to +0.12% and +0.91% [25]. The values obtained in the present work are –0.13% and –0.17%. Thus, aqueous cages of hydrates deform and "adjust" to the guest molecule. The interaction between water and gas molecules in the cage stabilizes water cells and prevents them from collapsing. To estimate the stabilization value quantitatively, we calculated binding energies between the gas molecule and the surrounding water framework.

BINDING ENERGY OF GASES IN HYDRATE CAGES

To calculate the binding energy of gas molecules in water cages (E_b) by the DFT method, the following quantities were found: total energy of an unfilled hydrate cell sI (E_c), total energy of the hydrate cell sI with various guest gases in D- and T-cages (E_{cm}), and energy of a free gas molecule (E_m). Then the binding energy was determined as:

$$E_b = E_{cm} - E_c - E_m. \quad (4)$$

For small CH_4, H_2S, H_2, N_2, Ar, Kr, Xe molecules, the binding energy in small D-cages is higher than that in large T-cages. Consequently, these gases stabilize better small cages. At the same time, larger CO_2, C_2H_6, C_3H_6 molecules better stabilize large T-cages. The binding energies calculated in the present work for CH_4, C_2H_6, C_3H_6 molecules in T-cages (–0.216 eV, –0.402 eV and –0.500 eV) (Table 2) agree well with values –0.244 eV, –0.375 eV, and –0.596 eV reported in [24]. The authors of [22] obtained binding energies of CO_2 and CH_4 gases in the D-cage: –2.36 eV and –0.58 eV, respectively. They differ from our calculations (–0.220 eV for CO_2 and –0.323 eV for CH_4), and the reason of these differences is probably due to the fact that the authors of [22] used the lattice parameter equal to 11.62 Å and assumed fixed environment in optimization calculations, while we used the value 12.03 Å from work [36] and taking into account the dynamics of all ions.

It is interesting how the binding energy depends on the masses and sizes of gas molecules and on their orientation relative to the water cell. Fig. 4 shows the binding energy as a function of the size of the hydrate-forming molecule; as can be seen, the binding energy increases together with the molecular diameter. The dependence of binding energy in aqueous cages on the weight of gas molecules (Fig. 5) shows that the binding energy increases with increasing molecular weight in a close to linear mode. Gases are divided into two groups according to the nature of the dependence of their binding energy in cages on the molecular mass: molecular ones and atomic ones (Fig. 5). For the first group, the coefficient of linear dependence is $dE_b/dM \in$ (–0.008; –0.006) eV·mol/g. For the second group formed by inert gases, $dE_b/dM \in$ (–0.002; –0.0015) eV·mol/g.

TABLE 2. Binding Energies of Gases in D- and T-Cages of the sI Hydrate. The Arrows Show Longitudinal and Transverse Orientations of Gas Molecules Relative to the Long Axis of the T-Cage

Gas	Cage	E_b, eV
CH_4	D	–0.323
CH_4	T	–0.216
H_2S	D	–0.481
H_2S	T	–0.352
H_2	D	–0.222
H_2	T	–0.134
N_2	D	–0.167
N_2	T	–0.124
Ar	D	–0.202
Ar	T	–0.116
Kr	D	–0.293
Kr	T	–0.193
Xe	D	–0.374
Xe	T	–0.252
CO_2	T(→)	–0.214
CO_2	T(↑)	–0.220
C_2H_6	T(→)	–0.373
C_2H_6	T(↑)	–0.402
C_3H_6	T(→)	–0.490
C_3H_6	T(↑)	–0.500

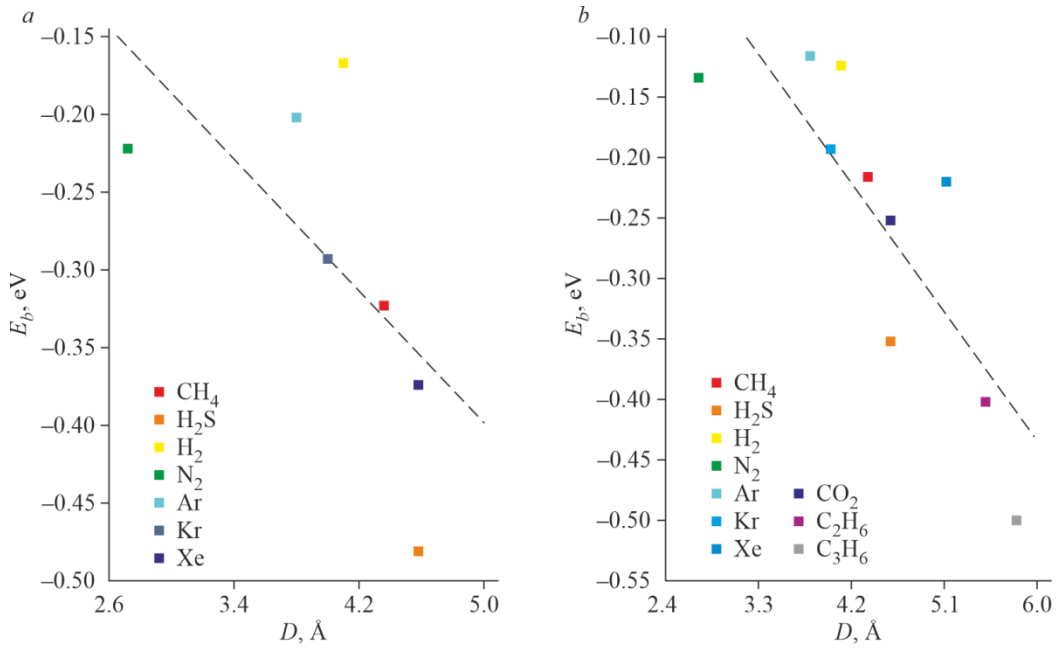

Fig. 4. Binding energies in D (*a*) and T (*b*) cages as functions of the gas molecule diameter.

The energy of interaction of a gas molecule with the water framework also depends on the molecule's orientation relative to the cage. This effect is quite small for a spherically symmetrical D-cage and is more pronounced for an ellipsoid T-cage. The T-cage is not spherical and is flattened from the sides of hexagonal faces (Fig. 6). As a result, various orientations of extended molecules such as CO_2, C_2H_6, C_3H_6 are characterized by different energies of interaction with the

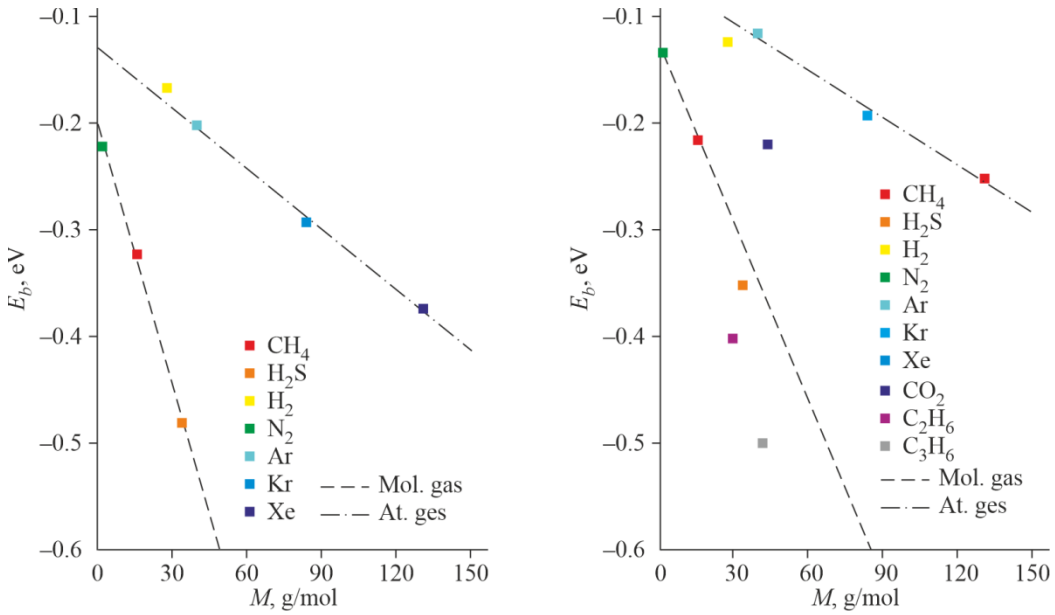

Fig. 5. Binding energies in D (*a*) and T (*b*) cages as functions of the gas molecular weight.

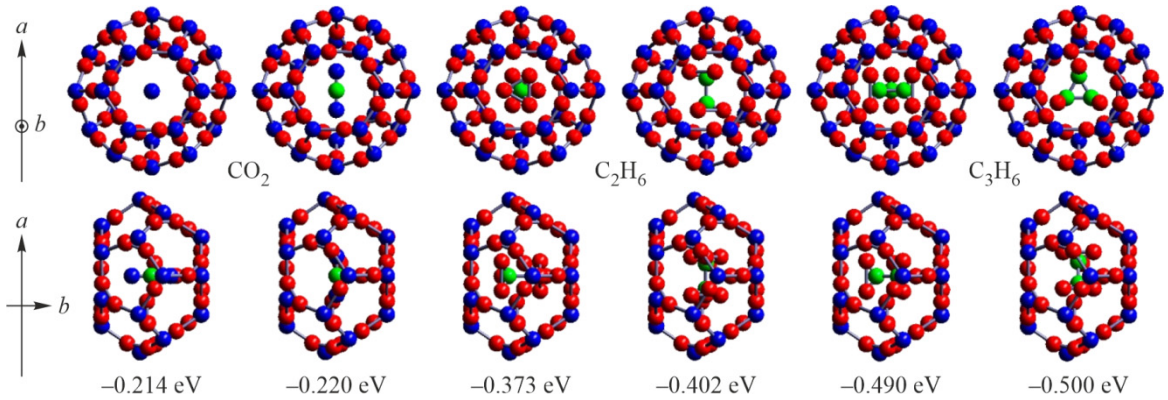

Fig. 6. Various orientations of non-spherical molecules CO_2, C_2H_6, and C_3H_6 in the hydrate T-cage and the corresponding binding energies E_b.

surrounding framework, as was confirmed by calculations. The orientation of CO_2 in the T-cage along the long axis *a* is energetically more favorable (by 0.006 eV or ≈3% of the binding energy) than along the short axis *b*. The orientation of C_2H_6 in the T-cage along the long axis *a* is more favorable by 0.03 eV (≈8% of the binding energy), and the orientation of C_3H_6 in the T-cage along the long axis *a* is more favorable by 0.01 eV (≈2% of the binding energy).

DENSITY OF ELECTRONIC STATES

The influence of guest gas molecules on the stability of sI hydrates was also studied by analysing the density of electronic states $N(E)$. Fig. 7 shows the $N(E)$ spectra of sI hydrates filled with methane and carbon dioxide and, for comparison, the $N(E)$ spectra of the unfilled sI lattice. The Fermi level corresponds to 0 eV. In the presence of CH_4 and CO_2 molecules, the electron density spectra contain characteristic peaks of *p*-electrons of carbon at –1.9 eV. The intensity of this peak for the methane hydrate is higher than that for the carbon dioxide hydrate, since the sI unit cell can encompass 8 CH_4 molecules and only 6 CO_2 molecules. Apparently, the peaks at –9 eV on the plot in Fig. 7*a* are related to the *s*-electrons of hydrogen of the methane molecules, while peaks at –5.5 eV in Fig. 7*b* correspond to the oxygen atoms of carbon dioxide. The band gap calculated for all the considered gases was found equal to ≈5.2 eV, meaning that the substance exhibits pronounced

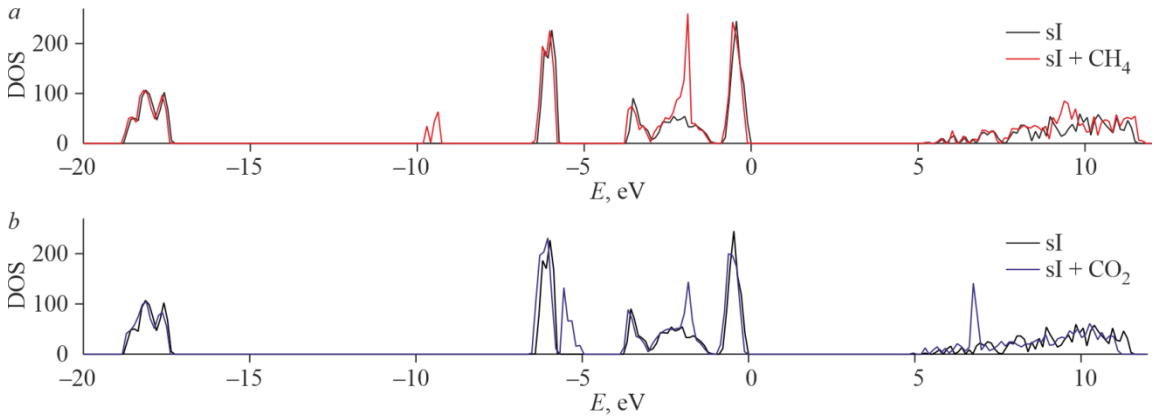

Fig. 7. Densities of electronic states $N(E)$ of unfilled hydrate sI, methane hydrate sI (*a*), and carbon dioxide hydrate (*b*).

dielectric properties. Besides, the band gap varies insignificantly depending on the hydrate-forming molecule. In both considered hydrates, the electron density is slightly shifted towards low energies when the cages contain gas molecules. This indicates that the electronic subsystem of the crystal structure occurs in a state with a lower energy. The presence of a gas molecule in the water framework increases the hydrate stability by reducing the total energy of the crystal. Despite the shift, the shape of the electron density distribution $N(E)$ of atoms constituting the water framework almost does not change.

CONCLUSIONS

In this work, stabilization of D- and T-cages of the sI-type gas hydrate by molecules of various gases was studied (CH_4, H_2S, H_2, N_2, Ar, Kr, Xe, CO_2, C_2H_6, C_3H_6). The influence of gas molecules on the geometry, binding energy, and density of electronic states of the hydrate crystal was considered using ab initio simulations. First, it was shown that guest gas molecules deform the cages and change their volumes. The guest molecule stabilizes the water cell and prevents it from collapsing. For the considered gases, the cage radius decrease from 0.04% to 0.23%. Second, we calculated the binding energies of hydrate-forming molecules in the D- and T-cages of the sI hydrate. It was found that molecules with a small diameter ($d < 5$ Å) better stabilize D-cages, while larger CO_2, C_2H_6, and C_3H_6 molecules with $d < 5$ Å better stabilize large T-cages. Third, we considered the dependence of the binding energy of gas molecules in the D- and T-cages on the mass, size, and orientation of the molecules. The binding energy increases with increasing molecular diameter. The binding energy also increases with increasing molecular weight in a close to linear mode. All gases can be conditionally referred to as molecular or atomic, depending on the type of their binding energy versus mass dependence. It was shown that different orientations of extended CO_2, C_2H_6, and C_3H_6 molecules in the non-spherical T-cage can be characterized by different binding energies, and the orientation of these molecules along the long axis is most preferable. Fourth, we obtained the density of electronic states $N(E)$ for the unfilled sI hydrate and for sI hydrates containing methane and carbon dioxide. It was found that the electron density of the hydrate is slightly shifted towards low energies in the presence of a guest molecule in the cage, indicating that the energy of the electronic subsystem decreases.

FUNDING

Large-scale quantum mechanical calculations were performed on the computing cluster of the Kazan (Volga Region) Federal University.

This work was funded by the Russian Science Foundation (project No. 22-22-00508).

CONFLICT OF INTERESTS

The authors declare that they have no conflicts of interests.

REFERENCES

1. E. D. Sloan and C. A. Koh. Clathrate Hydrates of Natural Gases. CRC Press, **2007**. https://doi.org/10.1201/9781420008494
2. Y. F. Makogon. Natural gas hydrates - a promising source of energy. *J. Nat. Gas Sci. Eng.*, **2010**, *2*, 45. https://doi.org/10.1016/j.jngse.2009.12.004
3. C. A. Koh, R. E. Westacott, W. Zhang, K. Hirachand, J. L. Creek, and A. K. Soper. Mechanisms of gas hydrate formation and inhibition. *Fluid Phase Equilib.*, **2002**, *194*, 143. https://doi.org/10.1016/S0378-3812(01)00660-4
4. F. A. Kuznetsov, V. A. Istomin, and T. V. Rodionova. Gazovye gidraty: istoricheskii ekskurs, sovremennoe sostoyanie, perspectivy issledovanii (Historical Survey, Present-Day State, Perspectives of Studies). *Ross. Khim. Zh.*, **2003**, *47*, 5. [In Russian]
5. F. Su, C. L. Bray, B. O. Carter, G. Overend, C. Cropper, J. A. Iggo, and A. I. Cooper. Reversible hydrogen storage in hydrogel clathrate hydrates. *Adv. Mater.*, **2009**, *21*, 2382. https://doi.org/10.1002/adma.200803402
6. V. A. Istomin and V. S. Yakushev. Gazovye gidraty v prirodnykh usloviyakh (Gas Hydrates in Natural Conditions). Moscow, Russia: Nedra, **1992**. [In Russian]
7. S. Sh. Byk, Y. F. Makogon, and V. I. Fomina. Gazovie gidraty (Gas Hydrates). Moscow, Russia: Himiya, **1980**. [In Russian]
8. A. G. Groysman. Teplofizicheskie svoistva gazovykh gidratov (Thermophysical Properties of Gas Hydrates). Novosibirsk, Russia: Nauka, **1985**. [In Russian]
9. C. A. Koh, E. D. Sloan, A. K. Sum, and D. T. Wu. Fundamentals and applications of gas hydrates. *Annu. Rev. Chem. Biomol. Eng.*, **2011**, *2*, 237. https://doi.org/10.1146/annurev-chembioeng-061010-114152
10. J. H. Van der Waals. The statistical mechanics of clathrate compounds. *Trans. Faraday Soc.*, **1956**, *52*, 184. https://doi.org/10.1039/TF9565200184
11. J. H. Van der Waals and J. C. Platteeuw. Validity of Clapeyron′s equation for phase equilibria involving clathrates. *Nature*, **1959**, *183*, 462. https://doi.org/10.1038/183462a0
12. W. F. Waite, L. A. Stern, S. H. Kirby, W. J. Winters, and D. H. Mason. Simultaneous determination of thermal conductivity, thermal diffusivity and specific heat in sI methane hydrate. *Geophys. J. Int.*, **2007**, *169*, 767. https://doi.org/10.1111/j.1365-246X.2007.03382.x
13. Y. P. Handa. A calorimetric study of naturally occurring gas hydrates. *Ind. Eng. Chem. Res.*, **1988**, *27*, 872. https://doi.org/10.1021/ie00077a026
14. W. Cai, X. Huang, and H. Lu. Instrumental Methods for Cage Occupancy Estimation of Gas Hydrate. *Energies*, **2022**, *15*, 485. https://doi.org/10.3390/en15020485
15. R. K. Zhdanov, V. R. Belosludov, Y. Y. Bozhko, O. S. Subbotin, K. V. Gets, and R. V. Belosludov. Thermodynamic description of crystalline water phases containing hydrogen. *JETP Lett*., **2018**, *108*, 806. https://doi.org/10.1134/S0021364018240128
16. R. M. Khusnutdinoff, R. R. Khayrullina, and M. B. Yunusov. Molekulyarno-dinamicheskie issledovaniya protsessa kristallizatsii i rosta gazovykh gidratov v silno pereokhlazhdennoi dvukhfaznoi sisteme “metan-voda” (Molecular Dynamics Studies of the Process of Crystallization and Growth of Gas Hydrates in a Strongly Supercooled Two-Phase System “Methane-Water”). *Fiz. Tv. Tela*, **2023**, *2*, 339. https://doi.org/10.21883/FTT.2023.02.54311.522 [In Russian]
17. L. C. Jacobson, W. Hujo, and V. Molinero. Thermodynamic stability and growth of guest-free clathrate hydrates: A low-density crystal phase of water. *J. Phys. Chem*., **2009**, *113*, 10298. https://doi.org/10.1021/jp903439a

18. Y. Bi and T. Li. Probing methane hydrate nucleation through the forward flux sampling method. *J. Phys. Chem*., **2014**, *118*, 13324. https://doi.org/10.1021/jp503000u
19. M. R. Walsh, G. T. Beckham, C. A. Koh, E. D. Sloan, D. T. Wu, and A. K. Sum. Methane hydrate nucleation rates from molecular dynamics simulations: Effects of aqueous methane concentration, interfacial curvature, and system size. *J. Phys. Chem*., **2011**, *115*, 21241. https://doi.org/10.1021/jp206483q
20. M. R. Walsh, C. A. Koh, E. D. Sloan, A. K. Sum. and D. T. Wu. Microsecond simulations of spontaneous methane hydrate nucleation and growth. *Science*, **2009**, *326*, 1095. https://doi.org/10.1126/science.1174010
21. V. R. Belosludov, K. V. Gets, R. K. Zhdanov, Y. Y. Bozhko, R. V. Belosludov, and L.-J. Chen. Collective Effect of Transformation of a Hydrogen Bond Network at the Initial State of Growth of Methane Hydrate. *JETP Lett.*, **2022**, *115*(3), 124-129. https://doi.org/10.1134/s0021364022030031
22. P. Guo, Y. L. Qiu, L. L. Li, Q. Luo, J. F. Zhao, and Y. K. Pan. Density functional theory study of structural stability for gas hydrate. *Chin. Phys. B*, **2018**, *27*, 043103. https://doi.org/10.1088/1674-1056/27/4/043103
23. Z. Wang, L. Yang, R. Deng, and Z. Yang. First-principle study on the electronic and optical properties of cages occupancy of SI methane hydrates. *arXiv.org, e-Print Arch., Condens. Matter*, **2019**, 1902.10914. https://doi.org/10.48550/arXiv.1902.10914
24. X. X. Cao, Y. Su, J. J. Zhao, C. L. Liu, and P. W. Zhou. Stability and Raman spectroscopy of alkane guest molecules (C_nH_m, $n \leq 6$, $m \leq 14$) in $5^{12}6^2$ and $5^{12}6^4$ water cages by density functional theory calculations. *Acta Phys. Sin*., **2014**, *63*, 1437. https://doi.org/10.3866/PKU.WHXB201405292
25. N. R. Sun, Z. W. Li, N. X. Qiu, X. H. Yu, X. R. Zhang, Y. J. Li, L. B. Yang, K. Luo, Q. Huang, and S. Y. Du. Ab initio studies on the clathrate hydrates of some nitrogen-and sulfur-containing gases. *J. Phys. Chem*., **2017**, *121*, 2620. https://doi.org/10.1021/acs.jpca.6b11850
26. M. B. Yunusov, R. M. Khusnutdinoff, and A. V. Mokshin. Electronic and thermophysical properties of gas hydrates: *Ab initio* simulation results. *Phys. Solid State*, **2021**, *63*, 372. https://doi.org/10.1134/S1063783421020268
27. M. B. Yunusov and R. M. Khusnutdinoff. First-principle molecular dynamics study of methane hydrate. *J. Phys. Conf. Ser*., **2022**, *2270*, 012052. https://doi.org/10.1088/1742-6596/2270/1/012052
28. L. Pauling and R. E. Marsh. The structure of chlorine hydrate. *PNAS*, **1952,** *38*, 112. https://doi.org/10.1073/pnas.38.2.112
29. M. Stackelberg and H. R. Muller. Feste Gashydrate II: Struktur und Raumchemie. *Z. Elektrochem. Angew.*, **1954**, *58*, 25. https://doi.org/10.1002/bbpc.19540580105
30. R. K. McMullan and G. A. Jeffrey. Polyhedral clathrate hydrates. IX. Structure of ethylene oxide hydrate. *J. Chem. Phys*., **1965**, *42*, 2725. https://doi.org/10.1063/1.1703228
31. T. C. Mak and R. K. McMullan. Polyhedral clathrate hydrates. X. Structure of the double hydrate of tetrahydrofuran and hydrogen sulfide. *J. Chem. Phys*., **1965**, *42*, 2732. https://doi.org/10.1063/1.1703229
32. J. A. Ripmeester, J. S. Tse, C. I. Ratcliffe, and B. M. Powell. A new clathrate hydrate structure. *Nature*, **1987**, *325*, 135. https://doi.org/10.1038/325135a0
33. R. M. Khusnutdinoff and A. V. Mokshin. Short-range structural transformations in water at high pressures. *J. Non-Cryst. Solids*, **2011**, *357*, 1677. https://doi.org/10.1016/j.jnoncrysol.2011.01.030
34. R. M. Khusnutdinoff and A. V. Mokshin. Vibrational features of water at the low-density/high-density liquid structural transformations. *Phys. A*, **2012**, *391*, 2842. https://doi.org/10.1016/j.physa.2011.12.037
35. R. M. Khusnutdinoff. Dynamics of a network of hydrogen bonds upon water electrocrystallization. *Colloid J*., **2013**, *75*, 792. https://doi.org/10.1134/S1061933X13060069
36. F. Takeuchi, M. Hiratsuka, R. Ohmura, S. Alavi, A. K. Sum, and K. Yasuoka. Water proton configurations in structures I, II, and H clathrate hydrate unit cells. *J. Chem. Phys*., **2013**, *138*, 124504. https://doi.org/10.1063/1.4795499
37. J. D. Bernal and R. H. Fowler. A theory of water and ionic solution, with particular reference to hydrogen and hydroxyl ions. *J. Chem. Phys*., **1933**, *1*, 515. https://doi.org/10.1063/1.1749327

38. P. Hohenberg and W. Kohn. Inhomogeneous electron gas. *Phys. Rev*., **1964**, *136*, B864. https://doi.org/10.1103/PhysRev.136.B864
39. W. Kohn and L. J. Sham. Self-consistent equations including exchange and correlation effects. *Phys. Rev*., **1965**, *140*, A1133. https://doi.org/10.1103/PhysRev.140.A1133
40. R. O. Jones and O. Gunnarsson. The density functional formalism, its applications and prospects. *Rev. Mod. Phys*., **1989**, *61*, 689. https://doi.org/10.1103/RevModPhys.61.689
41. K. Burke and L. O. Wagner. DFT in a nutshell. *Int. J. Quantum Chem.*, **2013**, *113*, 96. https://doi.org/10.1002/qua.24259
42. J. P. Perdew. K. Burke, and M. Ernzerhof. Generalized gradient approximation made simple. *Phys. Rev. Lett*., **1996**, *77*, 3865. https://doi.org/10.1103/PhysRevLett.77.3865
43. K. Berland, V. R. Cooper, K. Lee, E. Schroder, T. Thonhauser, P. Hyldgaard, and B. I. Lundqvist. Van der Waals forces in density functional theory: a review of the vdW-DF method. *Rep. Prog. Phys*., **2015**, *78*, 066501. https://doi.org/10.1088/0034-4885/78/6/066501
44. D. Chakraborty, K. Berland, and T. Thonhauser. Next-generation nonlocal van der Waals density functional. *J. Chem. Theory Comput*., **2020**, *16*, 5893. https://doi.org/10.1021/acs.jctc.0c00471
45. G. Kresse and J. Furthmuller. Efficient iterative schemes for ab initio total-energy calculations using a plane-wave basis set. *Phys. Rev. B*, **1999**, *54*, 11169. https://doi.org/10.1103/PhysRevB.54.11169
46. P. Pulay. Convergence acceleration of iterative sequences. The case of SCF iteration. *Chem. Phys. Lett*., **1980**, *73*, 393. https://doi.org/10.1016/0009-2614(80)80396-4
47. S. Y. Willow and S. S. Xantheas. Enhancement of hydrogen storage capacity in hydrate lattices. *Chem. Phys. Let*., **2012**, *525*, 13. https://doi.org/10.1016/j.cplett.2011.12.036